1Pa5-2

# Ultrasonic Measurement of Carotid Arterial Wall Thickness Applying Accurate Ultrasonic Measurement Method of Carotid Arterial Surface Roughness

Yoshifumi Nagai[1†], Shohei Mori[2], Mototaka Arakawa[1,2], and Hiroshi Kanai[2,1] ([1]Grad. School Biomed. Eng., Tohoku Univ.; [2]Grad. School Eng., Tohoku Univ.)

## 1. Introduction

In the diagnosis of arteriosclerosis, the thickness of the carotid arterial wall from the B-mode image obtained by the ultrasonic diagnostic device is widely used as one of the indexes. However, the B-mode image cannot capture local and minute thickness smaller than the pulse width. In addition to being affected by speckle noise in the body, quantization error occurs when converting to discrete data. Thus, the thickness of about several tens of μm [1], which is thought to occur in the early stage of arteriosclerosis, is difficult to measure.

In recent years, it has been confirmed that the carotid arterial wall is displaced in the longitudinal direction during one heartbeat. Using this longitudinal motion, methods for measuring the luminal surface roughness of the carotid arterial wall with high spatial resolution have been proposed [2].

In the present study, by applying this measurement method to the lumen-intima boundary (LIB) and the medial-adventitia boundary (MAB) of the carotid arterial wall, a novel method to measure the local and minute thickness of the carotid arterial wall is proposed.

## 2. Principles

In the present study, the surface profile is measured using the longitudinal displacement of the carotid arterial wall by the phased-tracking method and block matching [2]. At the 0-th frame, the depth of boundary to be measured is detected based on the amplitude of the echo. Figure 1 illustrates the detected depth of boundary, where the axial and lateral directions are shown by $z$-axis and $x$-axis in the space outside the body, respectively. $x_m(0)$ is the initial lateral position of the $m$-th ultrasonic beam on the boundary to be measured, $z_m(x_m(0))$ is the true depth of boundary at $x_m(0)$, and $\hat{z}_m(x_m(0))$ is the estimated depth of the boundary. Depth detection error $e_m$ such as quantization error occur as follows. (In some cases, a quantization error of about 10 μm may occur shown in Fig.1.)

$$e_m = \hat{z}_m\big(x_m(0)\big) - z_m\big(x_m(0)\big) \qquad m = 1,2,\ldots \tag{1}$$

The carotid arterial wall is displaced in the lateral direction between the $n$-th frame and the $(n+1)$-th frame. If the boundary to be measured has a roughness, the phase shift of the echo is caused by the displacement of the depth of the boundary. By detecting the phase shift of the echo, the axial displacement $\widehat{\Delta d_m}(n)$ of the $m$-th beam between the $n$-th frame and the $(n+1)$-th frame is obtained. The global lateral displacement $\Delta x(n)$ of the carotid arterial wall at $n$-th frame is estimated as $\Delta\hat{x}(n)$ by block matching, where it is assumed that the arterial wall does not expand or contract in the measurement region because the measurement region in the lateral direction is as small as 9 mm. At the lateral position $x' \equiv x_m(0) + \Delta\hat{x}(n)$, the depth $\hat{z}_m(x')$ of the boundary along the $m$-th ultrasonic beam at the $n$-th frame is obtained by accumulation $\sum_{n'=0}^{n} \widehat{\Delta d_m}(n')$ of instantaneous axial displacements $\widehat{\Delta d_m}(n)$ from the initial depth $z_m(x_m(0))$ as follows.

$$\begin{aligned}\hat{z}_m(x') &\equiv \hat{z}_m\big(x_m(0) + \Delta\hat{x}(n)\big)\\ &= z_m(x_m(0)) + \sum_{n'=0}^{n} \widehat{\Delta d_m}(n')\\ &= \hat{z}_m(x_m(0)) - e_m + \sum_{n'=0}^{n} \widehat{\Delta d_m}(n')\end{aligned} \tag{2}$$

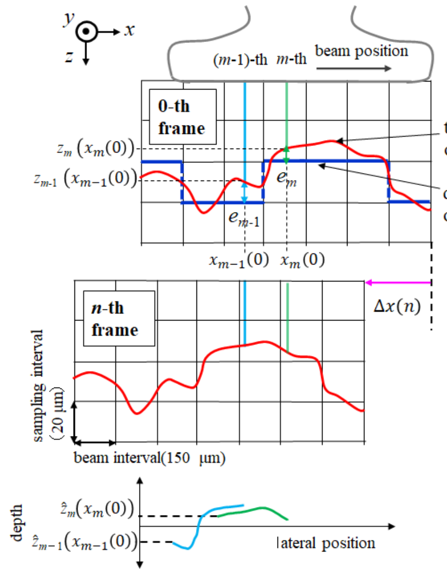


Fig.1. Illustration of measurement.

To correct the error $e_m$ that occurs for each beam, the initial depth $\hat{z}_m(x_m(0))$ should be adjusted. Since the longitudinal displacement of the carotid arterial wall is larger than the beam interval (150 μm), there is a region where the measurements overlap. The RMS error $\varepsilon_m(\alpha_m)$ is calculated for the overlapping region to find the adjustment amount

$\alpha_m$ for each profile $\hat{z}_m(x')$ measured by $m$-th beam. The minimum of the RMS error $\varepsilon_m(\alpha_m)$ for the optimal $\widehat{\alpha_m}$ is given by

$$\varepsilon_m(\widehat{\alpha_m}) = \sqrt{\frac{1}{N}\sum_{x'=0}^{N-1}\left(\hat{z}_m(x') - (\hat{z}_{m-1}(x') + \widehat{\alpha_{m-1}}) + \widehat{\alpha_m}\right)^2} \quad (3)$$

Here, $\widehat{\alpha_0} = 0$, and $N$ shows the number of the same lateral position data between the profile data measured by the $m$-th beam and $(m-1)$-th beam. In the region measured by multiple beams, the measured profiles obtained by multiple beams are averaged. The averaged depth $\hat{z}(x')$ of the boundary is given by

$$\hat{z}(x') = \frac{1}{\left(\frac{\Delta\hat{x}(n)}{d} + 1\right)} \sum_{i=m-\frac{\Delta\hat{x}(n)}{d}}^{m} (\hat{z}_i(x') + \hat{\alpha}_i) \quad (4)$$

Here, $d$ shows the ultrasonic beam interval. The procedure described above is applied to the LIB and MAB, the depths of these boundaries are measured as $\hat{z}_{\mathrm{LIB}}(x)$ and $\hat{z}_{\mathrm{MAB}}(x)$. The thickness $t(x)$ between measured profiles $\hat{z}_{\mathrm{LIB}}(x)$ and $\hat{z}_{\mathrm{MAB}}(x)$ is given by

$$t(x) = \hat{z}_{\mathrm{MAB}}(x) - \hat{z}_{\mathrm{LIB}}(x) \quad (5)$$

Thus, by the proposed method, unlike the conventional method (B mode image) in which the boundary is detected discretely at each beam position, the continuity of the boundary measured by adjacent beams is maintained by displacement measurements over time for multiple frames and using the overlapping region of measurement, and the quantization error in the axial direction that occurs discretely can be corrected.

## 3. Experiment

In the phantom experiment, a silicone phantom was used. It has two layers consisting of a silicone sheet with a thickness of 0.5 mm that simulates the intima-media complex and silicone rubber that simulates the adventitia. *In vivo* data was obtained from the carotid artery of a 33-year-old healthy male. The center frequency and sampling frequency were set to 7.5 MHz and 40 MHz, respectively, and the frame rate was set to 187 Hz.

In the B-mode image of the phantom shown in Fig. 2(A), the depths corresponding to the LIB and the MBA are shown by a red line and a blue line, respectively. These lines of boundaries were determined based on the amplitude, but partial discrete detections occur due to the influence of noise and quantization error. Fig. 2(B) shows the thickness by the conventional method (thickness obtained by finding the difference between the above-mentioned boundary depth detection results) and the proposed method. By the proposed method, it can be confirmed that the result by the proposed method is closer to the true value (0.5mm).

In the B-mode image of *in vivo* data shown in Fig. 3(A), the LIB and the MAB detected based on the amplitude are shown by a red line and a blue line. The discrete boundary depth detection error, which seems to be the effect of noise, can be confirmed in MAB. Fig. 3(B) shows the thickness obtained by the conventional method and the proposed method. By the proposed method, it can be confirmed that the measurement results are smoother.

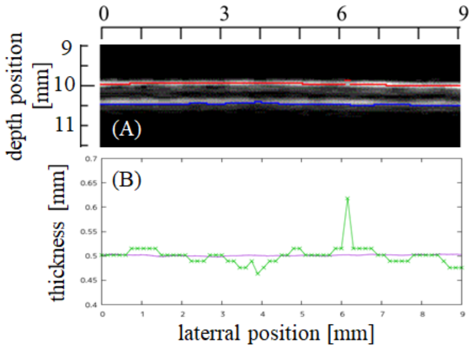


Fig. 2. (A) B-mode image of the phantom. (B) Measured thickness of phantom (proposed method: magenta, conventional method: green).

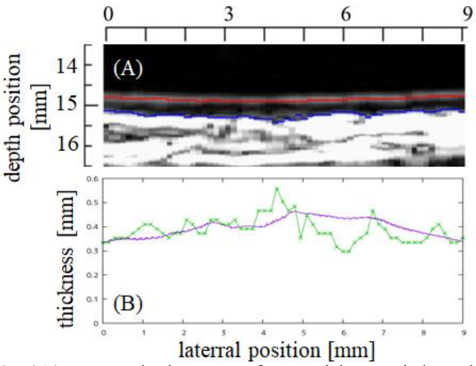


Fig. 3. (A) B-mode image of carotid arterial wall. (B) Measured thickness of carotid arterial wall (proposed method: magenta, conventional method: green).

## 4. Conclusion

In the present study, from the measurement results of the phantom, it was shown that the thickness measured by the proposed method is closer to the true value than the conventional method (B-mode image), and high-precision measurement is possible. Moreover, by applying the proposed method to *in vivo* data, it was confirmed that the thickness can be measured more smoothly than the conventional method.

## References


1. E. Sho, M. Sho, T. M. Singh, H. Nanjo, M. Komatsu, C. Xu, H. Masuda, and C. K. Zarins: Exp. Mol. Pathol. 73 (2002) 142.
2. K. Kitamura, H. Hasegawa, and H. Kanai: Jpn. J. Appl. Phys. 51 (2012) 07GF05-1.